Published in final edited form as:

Neuroimage. 2017 June ; 153: 189–197. doi:10.1016/j.neuroimage.2017.03.051.

Functional dynamics of hippocampal glutamate during associative learning assessed with in vivo ^{1}H functional magnetic resonance spectroscopy

Jeffrey A. Stanley[1], **Ashley Burgess**[1], **Dalal Khatib**[1], **Karthik Ramaseshan**[1], **Muzamil Arshad**[2,3], **Helen Wu**[2], and **Vabhav A Diwadkar**[1]

[1]Brain Imaging Research Division, Department of Psychiatry & Behavioral Neurosciences, Wayne State University School of Medicine, Detroit, MI

[2]Translational Neuroscience Program, Department of Psychiatry & Behavioral Neurosciences, Wayne State University School of Medicine, Detroit, MI

[3]Institute of Gerontology, Wayne State University, Detroit, MI

Abstract

fMRI has provided vibrant characterization of regional and network responses associated with associative learning and memory; however, their relationship to functional neurochemistry is unclear. Here, we introduce a novel application of *in vivo* proton functional magnetic resonance spectroscopy (^{1}H fMRS) to investigate the dynamics of hippocampal glutamate during paired-associated learning and memory in healthy young adults. We show that the temporal dynamics of glutamate differed significantly during processes of memory consolidation and retrieval. Moreover, learning proficiency was predictive of the temporal dynamics of glutamate such that fast learners were characterized by a significant increase in glutamate levels early in learning, whereas this increase was only observed later in slow learners. The observed functional dynamics of glutamate provides a novel *in vivo* marker of brain function. Previously demonstrated N-methyl-D-aspartate (NMDA) receptor mediated synaptic plasticity during associative memory formation may be expressed in glutamate dynamics, which the novel application of ^{1}H MRS is sensitive to. The novel application of ^{1}H fMRS can provide highly innovative vistas for characterizing brain function *in vivo*, with significant implications for studying glutamatergic neurotransmission in health and disorders such as schizophrenia.

*Corresponding Author. Jeffrey A. Stanley, Ph.D., Brain Imaging Research Division, Department of Psychiatry & Behavioral Neurosciences, Wayne State University School of Medicine, Detroit, MI, 48201. Tel.: 313.577.9090; Fax: 313.577.5900. jeffrey.stanley@wayne.edu.

Disclosure statement

The authors of this publication have no conflicts to disclose.

Supplementary — Caption to Figure

Supplement Figure 1: Mean % levels of hippocampal glutamate across each of the eight encoding (A) and retrieval (B) epochs for each of the learning groups (i.e., fast learners in blue and slow learners in red). Significant differences ($p<0.05$) in glutamate levels relative to the control condition are indicated for the fast (†) and slow (‡) learners.

Keywords

associative learning and memory; in vivo; glutamate; functional; MRS

1. Introduction

Glutamate is the brain's major excitatory neurotransmitter, and plays a particularly salient role in frontal-hippocampal mechanisms of learning and memory (Castner and Williams, 2007). The hippocampal formation is particularly rich in glutamatergic neurons, and hippocampal-based mechanisms of memory consolidation are presumed to be subserved by N-methyl-D-aspartate (NMDA) mediated synaptic plasticity (Bliss and Collingridge, 1993). NMDA is the principle ionotropic glutamate receptor; rodent studies have indicated that calcium flux through the NMDA receptor is principally implicated in learning and memory (Slutsky et al., 2004). Generally, the molecular and genetic bases of learning have been extensively studied in rodent models, yet methodological gaps limit translating mechanisms of action across species. Animal studies can rely on single or multi-unit neuronal recordings, or the use of genetic models of memory, via NMDA knockouts, that can be emulated in humans only under pre-surgical conditions (Suthana et al., 2015b). Thus animal studies provide valuable approximation of the *neurochemical* contributions to learning and memory (Chen and Tonegawa, 1997; Silva, 2003).

By comparison, *in vivo* human studies are largely forced to rely on hemodynamic (via the BOLD fMRI signal) rather than neurochemical signals to infer hippocampal function. fMRI has provided vibrant characterization of regional and network responses associated with associative learning and memory (Banyai et al., 2011; Ranganath et al., 2005; Sommer et al., 2005; Suthana et al., 2015a; Wadehra et al., 2013; Woodcock et al., 2015), but their relationship to functional neurochemistry is unclear at best (Logothetis, 2008). The use of *in vivo* signals that capture functional neurochemistry can provide a more direct assessment of neurochemical dynamics. Here, we provide novel application of proton *functional* magnetic resonance spectroscopy (^{1}H fMRS) to characterize *in vivo* glutamate dynamics during hippocampal-based associative learning. Previous ^{1}H fMRS studies have documented increased glutamate levels in response to visual stimulation (Bednařík et al., 2015b; Lin et al., 2012; Mangia et al., 2007; Mangia et al., 2006; Schaller et al., 2013) or during motor responding (Schaller et al., 2014). Notably however, these studies were conducted outside the hippocampus, and using non-glutamate reliant tasks. Here, we significantly expand on previous work with the first known demonstration of selective glutamate modulation in the hippocampus during associative learning and memory. These observations rest on the reasonable assumption that NMDA-driven hippocampal activity related to memory formation will lead to increased levels of glutamate in the hippocampus, an increase that the ^{1}H MRS signal will be sensitive to.

To establish the functional viability of ^{1}H fMRS, we specifically explored the temporal dynamics of the quantitated neurochemical signal as a function of learning proficiency on a paired-associated learning task. The course of paired-associate learning is well approximated by functions with a negatively accelerated or sigmoidal growth behavior, with limited free

parameters estimating learning rate (Diwadkar et al., 2008). The dynamics of the task thus permits cleavage into sub-groups of relatively fast and slow learners based on the fitted response functions, and task performance has been linked to estimated fMRI metrics. For instance, effective connectivity analyses of fMRI signals shows that the coupling of the hippocampus with specific heteromodal regions is statistically correlated with learning rates (Banyai et al., 2011), and generally, fMRI-characterized “neural” responses are predictive of subsequent remembering and forgetting of associated memories (Addante et al., 2015; Kim, 2011). These fMRI studies indicated that estimated amplitude of the fMRI BOLD response and hippocampal connectivity is yoked to behavioral proficiency.

In extending the linkage between performance and measures of brain function using ^{1}H fMRS characterized glutamate dynamics, we seek to a) establish the technique’s viability and specificity and b) present an expanded framework for *in vivo* assessment of hippocampal function (and dysfunction) in health and disorders providing a significant complement to fMRI.

We organize the presentation of our results in the following sequence in concert with our *a priori* goals:

1. First we present a comprehensive characterization of behavioral proficiency. These analyses show significant effects of time on performance, confirming the expected behavioral dynamics of the task. We next used the fitted performance functions to the behavioral results to cleave the participants into two sub-groups corresponding to fast and slow learners. This separation is logically connected with our subsequent presentation of the analyses of the ^{1}H fMRS data.
2. From the ^{1}H fMRS data we characterize effects of task condition (Encoding and Retrieval) and Time on modulated glutamate. These analyses establish significant effects of each of the task conditions and time on glutamate modulation. Next between fast and slow learners we demonstrate differences in the temporal dynamics of the glutamate response suggesting that the temporal dynamics of glutamate modulation in the hippocampus corresponds with behavioral proficiency.

2. Materials and Methods

2.1 Subjects

A total of 16 healthy, young adults (9 males; mean age of 25.0 ± 2.0 yrs.; 22-29.2 yrs.) were recruited through local advertisements at Wayne State University. All participants provided signed informed consent approved by the Wayne State University Institutional Review Board. Based on screening questionnaires, participants were free of past or current medical, psychiatric and/or neurological illness (e.g., hypertension, thyroid disease, diabetes, asthma requiring prophylaxis, seizures or significant head injury with loss of consciousness) and/or MRI contraindications.

2.2 Associative Learning/Memory fMRS Task

The ^{1}H fMRS data was collected while participants engaged in an associative learning and memory paradigm that required subjects to over time, learn the associations between objects and locations in space (Figure 1). Previous fMRI studies have shown that the task strongly modulates responses in the hippocampus, as well as effective connectivity between the hippocampus and neo-cortical regions (Banyai et al., 2011; Buchel et al., 1999; Woodcock et al., 2016; Woodcock et al., 2015). Moreover, behavioral proficiency on the task has been shown to conform to classic mechanisms of negatively accelerated learning (Diwadkar et al., 2016; Diwadkar et al., 2008), suggesting that the task characteristics strongly engage basic hippocampal mechanisms of learning and memory (Hasselmo, 1999; Rolls, 1996).

As shown in the task schematic in Figure 1, participants were required to learn nine object-location pairs over eight blocks, each of which cycled between encoding, rest, retrieval and rest epochs. During each encoding epoch, the nine equi-familiar objects (Snodgrass and Vanderwart, 1980) were present in randomized sequence in their associated grid location (3sec/object totaling 27sec). Participants were instructed to vocalize the name of the object as presented (monosyllabic object names minimized head motion; All responses were recorded through a microphone system as part of assessing performance). Following a brief rest/rehearsal epoch (27sec), cued retrieval was employed to test participant memory. The nine grid locations were cued (red square; 3sec/cue totaling 27sec) in random order, with participants instructed to respond by vocalizing the name of the object associated with the grid location (participants responded “no” if they could not recall or guess the associated object). The extended length of the task (eight blocks; 14:24 minutes), was designed to maximize the possibility of participants reaching asymptotic performance.

For each participant, behavioral data was collected during the cued-Retrieval epochs. For each participant, performance data (expressed as % correct) was modeled using a nonlinear least-square fitting algorithm of the Gompertz function (below; (Gompertz, 1825)). The Gompertz function optimizes three parameters that characterize sigmoidal behavior of the data: These are a) the asymptote (that can be construed as learning capacity), b) point of inflection in time (that can be construed of as when performance transitions to approach asymptote), and c) the learning rate time constant on the paradigm. In the equation below, time, is represented by the block number (Range: 1–8):

$$\%\mathrm{Correct}=\mathrm{Asymptote}\ ^{\cup}\mathrm{e}^{-(\mathrm{e}^{(-\frac{(\mathrm{time}-\mathrm{InflectionPoint})}{\mathrm{LeamingRate}})})}$$

Modeling of behavioral responses was conducted using the Isquonlin function in Matlab (The MathWorks, Inc.), which included imposing a lower bound limit of 0 for all three parameters and an upper bound limit of 100% for the asymptote parameter.

2.3 Baseline Control Condition

As our goal was to assess task-active modulation of glutamate in the hippocampus during a hippocampal-centric paradigm, we employed a non-hippocampal baseline task as a control condition. The simple uni-manual visuo-motor integration paradigm employed as the control

condition (Asemi et al., 2015) required participants to tap their forefinger and their thumb in response to a flashing visual stimulus. Cues were presented 0.5sec in duration at varying frequencies between 0.7Hz and 1.4Hz in which participants were instructed to tap their index finger and thumb together at each cue. A total of six finger-tapping epochs (34sec/epoch) interspersed with 20sec rest epochs were employed.

This control paradigm induces strong attention and motor processing, without learning or memory components. The task was administered before the learning paradigm to estimate modulation of hippocampal glutamate in an active control state. Subsequently, glutamate levels during learning were expressed relative to the levels during this finger tapping baseline task.

2.4 Functional Magnetic Resonance Spectroscopy (fMRS)

All MR imaging data was collected on a 3T Siemens Verio system using a 32-channel head-coil. A set of T_1-weighted axial images covering the whole brain was collected ($1mm^3$ pixel resolution) and images were resampled and used to prescribe the placement of a $1.7 \times 3.0 \times 1.2cm^3$ (or 6.12 cm^3) MRS voxel in the right anterior portion of the hippocampus (i.e., the location of the anterior edge of MRS voxel coincided with the anterior edge of the hippocampus and not include the amygdala). Angulation and rotation of the MRS voxel was allowed accordingly to minimize the partial volume effect (Figure 2). During the finger-tapping and learning/memory tasks, 22 individual and consecutive single-voxel, short-TE ^{1}H MRS measurements of 16 averages each were collected. The acquisition protocol included: point-resolved spectroscopy (PRESS) sequence with outer volume saturation (OVS) for improved localization precision and reduced signal contamination from outside the specified voxel, TR= 3.375s, TE= 23ms, 2,048 data points, 2kHz bandwidth,16 averages, acquisition time of 54s per measurement and VAPOR (Variable Power and Optimized Relaxation Delays) for water suppression and cleaner spectral baseline (Tkác and Gruetter, 2005). Selecting a short-TE minimized the signal attenuation due to T_2 relaxation (i.e., T_2-weightedness) and the J-modulation effects of coupled spins. Prior to each acquisition, the homogeneity of the magnetic field was optimized (or shimmed) using FASTESTMAP (Fast, Automatic Shim Technique using Echo-planar Signal readout for Mapping Along Projections)(Gruetter and Tk, 2000). A fully relaxed water-unsuppressed spectrum was also collected following the task (i.e., with a TR=10sec and 2 averages).

A main goal of this study was to assess changes in the levels of hippocampal glutamate *over time* for each *task condition* (encoding and retrieval epochs), therefore the 22 ^{1}H MRS measurements were binned based on task conditions. Moreover, the ^{1}H MRS measurements in successive task epochs were averaged in pairs (i.e., by signal averaging two successive spectra prior to spectral quantification), increasing the S/N ratio and permitting reliable quantification. The pairing scheme is illustrated in Figure 1B.

Post-processing and quantification of the ^{1}H MRS data was 100% automated. For each pair of averaged 1H MRS signal, the ^{1}H metabolites, glutamate, N-acetyl-aspartate (NAA), phosphocreatine plus creatine (PCr+Cr), trimethylamines [glycerophosphocholine plus phosphocholine (GPC+PC)], and *myo*-inositol, glutamine, taurine, N-acetyl-aspartylglutamate, alanine, aspartate, gamma-amino-butyric acid (GABA), and glucose, and

the lipid and macromolecule resonances (Seeger et al., 2003) were quantified using the Linear Combination (LC) Model software (Provencher, 1993) with simulated basis set for the *a priori* knowledge reflecting the acquisition parameters. A typical example of an individual ^{1}H MRS spectrum from the right hippocampus (head/body) is shown in Figure 2. Freesurfer and FSL tools (FLIRT, FAST, MRI_VOLSYNTH, MRI_VOL2VOL) were used to tissue segment the T_1-weighted images, which were then used to quantify the tissue fraction values within each voxel location. The absolute concentration of glutamate was estimated using the fully relaxed unsuppressed water signal, tissue fraction values and the appropriate T_1 and T_2 relaxation values as described by Gasparovic et al. (2006).

2.5 Statistical Analyses

To ensure analyses were comparable across the behavioral and fMRS data, the behavioral data (like the MRS data) were also averaged across successive pairs of epochs (see Figure 1B). For the behavioral analyses, % correct served as the dependent variable and paired epochs as the main term. Initial assessment of differences in glutamate levels between task conditions (Control, Encoding and Retrieval) was conducted with task condition as the main term, followed by post-hoc analyses. These analyses were conducted using the repeated measures generalized estimating equations (GEE) and differences of least squares means for post-hoc comparisons (SAS GENMOD; SAS Institute Inc.).

Additionally, the testing of differences in the temporal dynamics of glutamate modulation across the paired epochs for both the Encoding and Retrieval conditions was conducted using the repeated measure GEE statistics with epoch number as the main term followed by post-hoc comparisons. All GEE analyses included age and gender as covariates.

Investigating differences in sub-groups of learners was one of the central aims of the paper. To facilitate this, we applied a median split on the inflection parameter from the modeling of the behavioral data. As previously noted, the inflection parameter models the *transition* from linear to asymptotic performance: It is expected that faster learners will transition *earlier* from linear to asymptotic learning than slower learners. Considering the limited sample size and non-normal distribution in the data, nonparametric Wilcoxon tests (JMP; SAS Institute Inc.) were performed to assess sub-group differences in the modeled parameters of the behavioral data (inflection point, learning rate time constant and asymptote value). In each sub-group, nonparametric-paired comparisons (Wilcoxon) were also conducted to identify unique differences in glutamate modulation across the paired encoding and retrieval epochs relative to the control condition. Lastly, differences in the glutamate level between the two sub-groups across the paired encoding and retrieval epochs were tested using nonparametric Wilcoxon tests. A p-value of 0.0125 or less was noted as significant, which reflects correcting for multiple comparisons with 4 comparisons per condition.

3. Results

3.1 Behavioral Results

The overall response rate on retrieval trials was 98%, indicative of high compliance and marginal data loss. Based on the % correct in recalling the 9 object-location pairs, the

averaged performance significantly improved across blocks (χ^2= 14.24; p=0.0026) while following sigmoidal behavior. The post-hoc comparisons revealed significant changes in performance between adjacent paired epochs (1st vs 2nd pair, p<0.0001; 2nd vs 3rd pair, p=0.049; 3rd vs 4th pair, p=0.0024).

A median split based on the inflection time parameter from the Gompertz function cleaved the group into slow and fast learners (n=8 in each). The fast learners included 3 males and 5 females whereas 6 males and 2 females were in the slow learner group. The groups did not differ in age (24.5±1.6 vs 25.5±2.3 years). Figure 3 includes a boxplot of the modeled parameters of the sub-groups, showing fast learners had both significantly earlier inflection times (0.53±0.41 vs 2.4±0.9; p<0.0001) and significantly faster learning rates (or smaller time constants; 0.99±0.44 vs 1.9±0.9; p=0.018). However, the two sub-groups asymptoted at the same level (89%±16% vs 95%±9%; p=0.60). Figure 4 provides a comprehensive accounting of behavioral proficiency and across sub-groups, the latter accentuating the differences in the inflection time and learning rates.

3.2 ^{1}H fMRS Results

The signal averaging of the acquired ^{1}H MRS data into paired ^{1}H MRS spectra was warranted, as it resulted in an ~33% improvement in the mean S/N ratio (±SD; 6.4±1.0 to 8.5±1.4). The confidence in quantifying glutamate in the paired ^{1}H MRS spectra ranged with Cramer-Rao lower bound (CRLB) values between 5% and 12% (mean±SD; 7.4±1.3%). The mean full-width-at-half-maximum (±SD) was 8.4±2.1Hz (range of 4.4Hz to 14.7Hz). All of the ^{1}H MRS data from the 16 subjects was used in the statistical analyses except for two paired ^{1}H MRS spectra, which were excluded due to CRLB values > 16% for glutamate (i.e., the absolute CRLB of glutamate was > 2 SD of the mean). The mean coefficient of variation (CV) of glutamate during the control baseline condition was 7.8%. Additionally, regarding the consistency in placing the ^{1}H MRS voxel in the head/body of the right hippocampus between subjects, the tissue segmentation of the ^{1}H MRS voxel resulted in a mean grey matter fraction (±SD) of 68.9%±4.2% (range of 61.5% to 74.4%).

3.2.1 Glutamate modulation by task condition and over time in the entire sample—

The associative learning task resulted in significant modulation of hippocampal glutamate (χ^2= 12.80; p= 0.0017; Figure 5), with the effects significant for each of the encoding (p< 0.0001) and retrieval (p= 0.0002) epochs compared to the control condition. Moreover, the task-effect on the neurochemistry was specific to glutamate evidenced by the lack of significance in the other quantitated metabolites including NAA (χ^2= 3.25; p= 0.20), PCr+Cr (χ^2= 3.38; p= 0.18), GPC+PC (χ^2= 2.71; p= 0.26) and myo-inositol (χ^2= 2.23; p= 0.33) as well as in the S/N (χ^2= 5.33; p= 0.070) and full-width-at-half-maximum (χ^2= 5.26; p= 0.072).

In the next statistical model we evaluated dynamic changes in glutamate levels across the four epoch pairs (see Figure 1) during encoding and retrieval. In these analyses time or the epoch term was significant for both encoding (χ^2= 13.41; p=0.0094) and retrieval (χ^2= 0.027). Post-hoc analyses showed significant increases of 7.1% (p=0.0014) and 4.5% (0.0009) in the glutamate modulation at the 1st and 2nd epoch pairs of encoding compared to

the control condition and the Cohen's d effect sizes were 0.82 and 0.60, respectively (Figure 6a). Glutamate levels tended to show an increase of 5.2% at the 4th epoch pair of encoding with an effect size of 0.63 but failed to reach significance (p=0.020). By comparison, post-hoc analyses showed a significant increase of 9.8% in glutamate only at the 3rd epoch pair of retrieval (p<0.0001) and the Cohen's d effect size was 1.1 (Figure 6b).

3.2.2 Glutamate dynamics vs learning proficiency in the sub-groups—Based on non-parametric paired comparisons, glutamate levels in the faster learning group showed a significant increase of 11% at the 1st paired epoch of encoding compared to the control condition (p=0.0096), whereas levels in the slower learning group displayed a significant increase of 7.7% at the 2nd paired epoch of encoding (p=0.0090) compared to the control condition (Figure 7A). The 8.2% glutamate increase at the 4th paired epoch of encoding in the slow learners failed to reach significance compared to the control condition(p=0.025). Glutamate levels in both learning sub-groups showed increased levels of 8.3% (p=0.048) and 11% (p=0.0025) respectively at the 3rd paired epoch of retrieval, both compared to the control condition but only reached significance for the slow learners (Figure 7B). Moreover, in directly comparing the % change in glutamate levels (relative to the control condition) between the two sub-groups, the slower learning group showed a significant increase at the 2nd paired epoch of encoding compared to the faster learning group (7.7% vs 1.3%; p=0.010) (Figure 7A).

4. Discussion

In this study we unveil the use of ^{1}H fMRS as a method for assessing specific aspects of brain function based on neurochemical signals, specifically glutamate modulation in the hippocampus. The viability of the method was tested in three ways: 1) First we induced hippocampal activity using a reliable paired-associate learning paradigm that fMRI studies have indicated provides highly reliable activity and dynamics of the hippocampus; 2) To test the specificity of the ^{1}H fMRS, we also contrasted the glutamate modulation in the hippocampus using a non-hippocampal visuo-motor paradigm; 3) Finally, to assess the behavioral relevance of ^{1}H fMRS, we assessed changes in glutamate levels as a function of learning proficiency, and whether glutamate dynamics differed between fast and slow learners.

Our results were these: 1) First, we provide the only documented *in vivo* evidence of glutamate modulation in the hippocampus during learning (Figure 5); 2) Second, with the relatively high temporal resolution of the *in vivo* hippocampal glutamate measurements we observed unique temporal dynamics of glutamate that differentiated between processes of memory formation (encoding) and retrieval (Figure 6); 3) Third, learning proficiency statistically predicted the temporal dynamics of glutamate: Fast learners were characterized by an early peak in modulated glutamate during encoding (Figure 7), whereas slow learners evinced a complimentary pattern.

In the remainder of this report, we discuss the methodological implications of using ^{1}H fMRS to asses *in vivo* function and neurochemical dynamics, and also unpack our observed effects in relating glutamate modulation to learning proficiency. We also discuss the general

value of the discriminative glutamate signal for *in vivo* characterization of NMDA-driven hippocampal function or dysfunction related to memory formation in health and disorders.

4.1 Putative mechanisms underpinning observed glutamate modulation

Glutamate plays a major role as an excitatory neurotransmitter in the cerebral cortex including the hippocampus (Erecinska and Silver, 1990), and NMDA receptor function is central in mediating synaptic plasticity necessary for learning and memory formation (Day et al., 2003). Following the neurotransmitter release of glutamate from the presynaptic terminal to the synaptic cleft, excess glutamate is taken up by surrounding astrocytes and subsequently converted predominantly to glutamine by glutamate synthase. Studies have shown a near 1:1 relationship between neuronal glucose oxidation and the glutamate-glutamine cycling (Rothman et al., 2003; Shen et al., 1999; Sibson et al., 1998), implying that the metabolic and neurotransmitter pool of glutamate, as typically viewed in the ^{1}H MRS literature (Berg and Garfinkel, 1971; Erecinska and Silver, 1990), are tightly coupled and hence, indistinguishable (Rothman et al., 2003). Thus, extant evidence suggests that task-active characterization of hippocampal glutamate must be directly related to neurontransmitter release induced by behavioral processing. We suggest that the demands of memory consolidation, lead to increased neuronal activity in the hippocampus, in turn leading to increased glucose utilization and oxidative metabolism (including increased glutamate-glutamine cycling). In response to memory formation, the increased levels of glutamate in the hippocampus is suggestive to be driven by the influx of oxidative metabolism related to increased neuronal activity (Mangia et al., 2012; Schaller et al., 2014). As is frequently employed in fMRI analyses, the contrast with a hippocampal-neutral condition, provides evidence of the selective modulation of glutamate by task.

4.2 Behavioral and glutamate dynamics in fast and slow learners

Performance on the object-location memory recall improved significantly over time characterized by sigmoidal behavior that reached an asymptote of 89% correct (±SEM of 3%). However, the expected high variability in performance across individuals (Figures 3 and 4), enabled the *a priori* goal of investigating the relationship between learning proficiency and the dynamics of the functional neurochemistry. Thus, whereas fast and slow learners did not differ in terms of learning “capacity” (the asymptote in each sub-group was at ~89% performance), both sub-groups differed in the modeled inflection point of their response functions. Fast learners reached 92% of their learning capacity by the third epoch (i.e., the mean performance was 82% correct by epoch #3), whereas the slow learners only reached 56% of their capacity by that time (Figures 3 and 4). When considered against the suggested mechanisms of glutamate modulation above, the distinction in the temporal course of learning between sub-groups assumes significance. Fast learners appear to engage in *earlier* successful memory consolidation than slow learners. Next, we discuss the relationship between the behavioral dynamics of the task in fast and slow learners, and neurochemical dynamics of glutamate.

Independent of time quantitated hippocampal glutamate increased significantly across all subjects during both encoding (5.2% relative to the motor control) and retrieval (4.2% relative to the motor control)(7 5). Increased glutamate was observed across three of the four

averaged encoding epoch pairs, but effects were more sporadic for retrieval pairs (Figure 6). Moreover, the variability in these effects appear to be related to temporal differences between the learning sub-groups (see more below). The relative specificity of the effects for encoding suggests some degree of preferential modulation of glutamate during memory *formation.* This may reflect the sensitivity of the NMDA-driven hippocampal modulation of glutamate in differentiating neural processes of memory formation from process of memory retrieval (see Woodcock et al., 2015 for fMRI based evidence of network differences between memory formation and retrieval).

As noted above, amongst fast learners, the sharpest increase in memory proficiency was achieved between the first and the second encoding epochs (Figure 4B). Notably, it was specifically in epochs one and two that fast learners showed a significant increase in glutamate levels (10.9% increase relative to the motor control condition), but slow learners did not (Figure 6). These effects emphasize the value of early hippocampal engagement during memory consolidation, reinforcing the idea that rapid consolidation is associated with early functional engagement of the hippocampus. These effects are consistent with molecular and lesion studies reiterating the importance of the *early* hippocampal involvement in memory formation subserving newly acquired behaviors (Wirth et al., 2003; Fyhn et al., 2002). Whereas we lack ^{1}H fMRS data to assert this, it is plausible that rapid learners are characterized by more rapid transition to shared hippocampal — neocortical memory representations (Haist et al., 2001; Eichennbaum, 2004). Finally, our previous analyses of fMRI data in an independent sample have shown that learning rate is positively correlated with the effective connectivity between the hippocampus and the prefrontal cortex (Banyai et al., 2011). In comparison to fast learners, in slow learners significant glutamate increases were not observed till the second pair of encoding epochs and were largely sustained (~7–8% increases over the motor control condition) through the remainder of the learning run (Figure 7).

Glutamate during memory retrieval evinced a different dynamic profile than encoding, and was not sensitive in distinguishing between sub-groups. Both sub-groups showed increased hippocampal glutamate levels in the third paired epoch (8.2% and 11.3%, respectively) with no other significant effects (Figure 7). This lack of effect on hippocampal glutamate is notable because of the presumed differences in hippocampal function during memory formation and retrieval. Whereas hippocampal neurons are central in initiating the formation of new memories (see Basu & Sieglebaum, 2015 for a recent review), neurons in the prefrontal cortex are assumed to assert greater relevance during memory retrieval (Tomita et al., 1999; Zhang and Williams, 2015). When assessed at the scale of macroscopic brain network interactions based on fMRI signals, retrieval cues induce prefrontal cortex driven interactions with the hippocampus (Woodcock et al., 2015; Simons and Spiers, 2003) resulting in substantial directional effects. These studies imply that during retrieval, the hippocampus may be the target of excitatory top-down inputs from the prefrontal cortex, as opposed to the source (which is the case during encoding). Future ^{1}H MRS assessments targeting the prefrontal cortex will be needed to assess the functional neurochemical signatures of these proposed effects.

4.3 Observed estimates of glutamate in recent context

The use of the FASTESTMAP method for shimming (Gruetter and Tk, 2000) as well as having effective OVS and VAPOR for water suppression (Tkác and Gruetter, 2005) were critical elements in acquiring high-quality ^{1}H MRS data from the hippocampus at a reasonable temporal resolution (54 s), given the difficulties of shimming due to significant susceptibility effects (Bednarík et al., 2015a). This led to an overall spectral quality that was comparable to published 3T ^{1}H MRS studies of the hippocampus (Allaïli et al., 2015; Bednařík et al., 2015a), as assessed by the CRLB values reflecting the confidence in quantifying glutamate, S/N and spectral linewidths.

The estimated mean concentration of glutamate in the hippocampus for the control condition was I3.4μmol/g, which is consistent with previous reports (Kassem and Bartha, 2003) including a recent study reporting a mean value of 14.3μmol/g in the hippocampus at 7 Tesla (Cai et al., 2013). The mean metabolite ratio of glutamate over glutamine was 3.2±0.9 for the control condition, which is also within the middle range of published studies (Govindaraju et al., 2000; Tkác and Gruetter, 2005) and provides additional support for the viability of accurately quantifying glutamate. The concentration of glutamate has also been noted to be higher in hippocampus compared to the cortex (Harris et al., 2014; Kassem and Bartha, 2003), which is expected given the high density of NMDA receptors in the structure. Interestingly, the magnitude change of the hippocampal glutamate of approximately 1.1 μmol/g to 1.5 μmol/g (or 8% to 11%) in response to the associative learning and memory is greater than the reported modulation of glutamate of approximately 0.2μmol/g (or 2% to 4%) in the cortex (Bednarík et al., 2015b; Lin et al., 2012; Mangia et al., 2007; Mangia et al., 2006; Schaller et al., 2013; Schaller et al., 2014), further highlighting the sensitivity of our measurements to the induced task. Though the relationship between the density of NMDA receptors and the task induced changes in glutamate is poorly understood, these differences between studies may be task or more importantly region specific.

5. Conclusions

We provide using *in vivo* ^{1}H fMRS novel evidence for dynamic glutamate modulation in the hippocampus during paired-associated learning and memory. Unique temporal dynamics of glutamate were associated with distinct processes of memory consolidation and retrieval, with the relatively high temporal resolution *in vivo* glutamate measurements. Further specificity was observed wherein learning proficiency predicted the temporal dynamics of glutamate during encoding such that fast learners were characterized by an *early* increase in glutamate levels but slow learners evinced increased glutamate levels *later* during encoding. Though the origins of the ^{1}H MRS signal are cumulative, the observed functional dynamics of glutamate is consistent with hippocampal-based mechanisms of memory consolidation subserved by NMDA receptor mediated synaptic plasticity. Moreover, ^{1}H MRS provides a potentially valuable complement to fMRI for focused exploration of *in vivo* brain function. Though further studies are warranted, these results provide a compelling and viable framework for the investigation of hippocampal (dys)function related to glutamatergic neurotransmission in heath and disorders using the novel application of ^{1}H fMRS.

Supplementary Material

Refer to Web version on PubMed Central for supplementary material.

Acknowledgments

Many thanks to Caroline Zajac-Benitez and Usha Rajan for their time and effort in assessing the participants and helping with the data processing. This work was supported by the National Institutes of Mental Health (1R01 MH111177 to J.A.S. and V.A.D.), the Mark Cohen Neuroscience Endowment and the Lycaki-Young Funds from the State of Michigan.

References

Addante RJ, de Chastelaine M, Rugg MD. Pre-stimulus neural activity predicts successful encoding of inter-item associations. NeuroImage. 2015; 105:21–31. [PubMed: 25450109]

Allaïli N, Valabrègue R, Auerbach EJ, Guillemot V, Yahia-Cherif L, Bardinet E, Jabourian M, Fossati P, Lehéricy S, Marjańska M. Single-voxel 1H spectroscopy in the human hippocampus at 3 T using the LASER sequence: characterization of neurochemical profile and reproducibility. NMR Biomed. 2015; 28:1209–1217. [PubMed: 26282328]

Asemi A, Ramaseshan K, Burgess A, Diwadkar VA, Bressler SL. Dorsal anterior cingulate cortex modulates supplementary motor area in coordinated unimanual motor behavior. Front Hum Neurosci. 2015; 9:309. [PubMed: 26089783]

Banyai M, Diwadkar VA, Erdi P. Model-based dynamical analysis of functional disconnection in schizophrenia. NeuroImage. 2011; 58:870–877. [PubMed: 21726653]

Bednařík P, Moheet A, Deelchand DK, Emir UE, Eberly LE, Bareš M, Seaquist ER, Öz G. Feasibility and reproducibility of neurochemical profile quantification in the human hippocampus at 3T. NMR Biomed. 2015a; 28:685–693. [PubMed: 25904240]

Bednařík P, Tkac I, Giove F, Dinuzzo M, Deelchand DK, Emir UE, Eberly LE, Mangia S. Neurochemical and BOLD responses during neuronal activation measured in the human visual cortex at 7 Tesla. Journal of Cerebral Blood Flow & Metabolism. 2015b; 35:601–610. [PubMed: 25564236]

Berg, CJvd, Garfinkel, D. A stimulation study of brain compartments. Metabolism of glutamate and related substances in mouse brain. Biochem J. 1971; 123:211–218. [PubMed: 5164952]

Bliss TV, Collingridge GL. A synaptic model of memory: long-term potentiation in the hippocampus. Nature. 1993; 361:31–39. [PubMed: 8421494]

Buchel C, Coull JT, Friston KJ. The predictive value of changes in effective connectivity for human learning. Science. 1999; 283:1538–1541. [PubMed: 10066177]

Cai K, Singh A, Roalf DR, Nanga RPR, Haris M, Hariharan H, Gur R, Reddy R. Mapping glutamate in subcortical brain structures using high-resolution GluCEST MRI. NMR Biomed. 2013; 26:1278–1284. [PubMed: 23553932]

Castner SA, Williams GV. Tuning the engine of cognition: a focus on NMDA/D1 receptor interactions in prefrontal cortex. Brain Cogn. 2007; 63:94–122. [PubMed: 17204357]

Chen C, Tonegawa S. Molecular genetic analysis of synaptic plasticity, activity-dependent neural development, learning, and memory in the mammalian brain. Annu Rev Neurosci. 1997; 20:157–184. [PubMed: 9056711]

Day M, Langston R, Morris RGM. Glutamate-receptor-mediated encoding and retrieval of paired-associate learning. Nature. 2003; 424:205–209. [PubMed: 12853960]

Dienel GA. Fueling and imaging brain activation. ASN NEURO. 2012; 4

Diwadkar VA, Bellani M, Ahmed R, Dusi N, Rambaldelli G, Perlini C, Marinelli V, Ramaseshan K, Ruggeri M, Bambilla P. Chronological age and its impact on associative learning proficiency and brain structure in middle adulthood. Behav Brain Res. 2016; 297:329–337. [PubMed: 26462573]

Diwadkar VA, Flaugher B, Jones T, Zalanyi L, Ujfalussy B, Keshavan MS, Erdi P. Impaired associative learning in schizophrenia: behavioral and computational studies. Cogn Neurodyn. 2008; 2:207–219. [PubMed: 19003486]

Erecinska M, Silver IA. Metabolism and role of glutamate in mammalian brain. Prog Neurobiol. 1990; 35:245–296. [PubMed: 1980745]

Gasparovic C, Song T, Devier D, Bockholt HJ, Caprihan A, Mullins PG, Posse S, Jung RE, Morrison LA. Use of tissue water as a concentration reference for proton spectroscopic imaging. Magnetic Resonance in Medicine. 2006; 55:1219–1226. [PubMed: 16688703]

Gompertz B. On the nature of the function expressive of the law of human mortality, and on a new mode of determining the value of life contingencies. Philosophical Transactions of the Royal Society of London. 1825; 115:513–583.

Govindaraju V, Young K, Maudsley AA. Proton NMR chemical shifts and coupling constants for brain metabolites. NMR Biomed. 2000; 13:129–153. [PubMed: 10861994]

Gruetter R, Tk I. Field mapping without reference scan using asymmetric echo-planar techniques. Magnetic resonance in medicine: official journal of the Society of Magnetic Resonance in Medicine / Society of Magnetic Resonance in Medicine. 2000; 43:319–323.

Harris JL, Yeh HW, Swerdlow RH, Choi IY, Lee P, Brooks WM. High-field proton magnetic resonance spectroscopy reveals metabolic effects of normal brain aging. Neurobiology of Aging. 2014; 35:1686–1694. [PubMed: 24559659]

Hasselmo ME. Neuromodulation and the hippocampus: memory function and dysfunction in a network simulation. Prog Brain Res. 1999; 121:3–18. [PubMed: 10551017]

Kassem MNE, Bartha R. Quantitative proton short-echo-time LASER spectroscopy of normal human white matter and hippocampus at 4 Tesla incorporating macromolecule subtraction. Magnetic resonance in medicine: official journal of the Society of Magnetic Resonance in Medicine / Society of Magnetic Resonance in Medicine. 2003; 49:918–927.

Kim H. Neural activity that predicts subsequent memory and forgetting: a meta-analysis of 74 fMRI studies. NeuroImage. 2011; 54:2446–2461. [PubMed: 20869446]

Lin Y, Stephenson MC, Xin L, Napolitano A, Morris PG. Investigating the metabolic changes due to visual stimulation using functional proton magnetic resonance spectroscopy at 7T. Journal of cerebral blood flow and metabolism : official journal of the International Society of Cerebral Blood Flow and Metabolism. 2012; 32:1484–1495.

Logothetis NK. What we can do and what we cannot do with fMRI. Nature. 2008; 453:869–878. [PubMed: 18548064]

Mangia S, Giove F, Dinuzzo M. Metabolic pathways and activity-dependent modulation of glutamate concentration in the human brain. Neurochemical Research. 2012; 37:2554–2561. [PubMed: 22846967]

Mangia S, Tkac I, Gruetter R, Van De Moortele PF, Maraviglia B, Uğurbil K. Sustained neuronal activation raises oxidative metabolism to a new steady-state level: evidence from 1H NMR spectroscopy in the human visual cortex. Journal of cerebral blood flow and metabolism : official journal of the International Society of Cerebral Blood Flow and Metabolism. 2007; 27:1055–1063.

Mangia S, Tkác I, Gruetter R, Van De Moortele PF, Giove F, Maraviglia B, Uğurbil K. Sensitivity of single-voxel 1H-MRS in investigating the metabolism of the activated human visual cortex at 7 T. Magnetic Resonance Imaging. 2006; 24:343–348. [PubMed: 16677939]

McKenna MC. Glutamate pays its own way in astrocytes. Frontiers in endocrinology. 2013; 4:191. [PubMed: 24379804]

Mergenthaler P, Lindauer U, Dienel GA, Meisel A. Sugar for the brain: the role of glucose in physiological and pathological brain function. Trends in Neurosciences. 2013; 36:587–597. [PubMed: 23968694]

Provencher SW. Estimation of metabolite concentrations from localized in vivo proton NMR spectra. Magnetic Resonance in Medicine. 1993; 30:672–679. [PubMed: 8139448]

Ranganath C, Heller A, Cohen MX, Brozinsky CJ, Rissman J. Functional connectivity with the hippocampus during successful memory formation. Hippocampus. 2005; 15:997–1005. [PubMed: 16281291]

Rolls ET. The orbitofrontal cortex. Philos Trans R Soc Lond B Biol Sci. 1996; 351:1433–1443. [PubMed: 8941955]

Rothman DL, Behar KL, Hyder F, Shulman RG. In vivo NMR studies of the glutamate neurotransmitter flux and neuroenergetics: implications for brain function. Annual review of physiology. 2003; 65:401–427.

Schaller B, Mekle R, Xin L, Kunz N, Gruetter R. Net increase of lactate and glutamate concentration in activated human visual cortex detected with magnetic resonance spectroscopy at 7 tesla. Journal of neuroscience research. 2013; 91:1076–1083. [PubMed: 23378234]

Schaller B, Xin L, O'Brien K, Magill AW, Gruetter R. Are glutamate and lactate increases ubiquitous to physiological activation? A (1)H functional MR spectroscopy study during motor activation in human brain at 7Tesla. NeuroImage 93 Pt. 2014; 1:138–145.

Seeger U, Klose U, Mader I, Grodd W, Nagele T. Parameterized evaluation of macromolecules and lipids in proton MR spectroscopy of brain diseases. Magn Reson Med. 2003; 49:19–28. [PubMed: 12509816]

Shen J, Petersen KF, Behar KL, Brown P, Nixon TW, Mason GF, Petroff OA, Shulman GI, Shulman RG, Rothman DL. Determination of the rate of the glutamate/glutamine cycle in the human brain by in vivo 13C NMR. Proc Natl Acad Sci U S A. 1999; 96:8235–8240. [PubMed: 10393978]

Shepherd, GM. Neurobiology. 3rd. Oxford University Press; New York: 1994.

Sibson NR, Dhankhar A, Mason GF, Rothman DL, Behar KL, Shulman RG. Stoichiometric coupling of brain glucose metabolism and glutamatergic neuronal activity. Proc Natl Acad Sci U S A. 1998; 95:316–321. [PubMed: 9419373]

Silva AJ. Molecular and cellular cognitive studies of the role of synaptic plasticity in memory. J Neurobiol. 2003; 54:224–237. [PubMed: 12486706]

Slutsky I, Sadeghpour S, Li B, Liu G. Enhancement of synaptic plasticity through chronically reduced Ca2+ flux during uncorrelated activity. Neuron. 2004; 44:835–849. [PubMed: 15572114]

Snodgrass JG, Vanderwart M. A standardized set of 260 pictures: norms for name agreement, image agreement, familiarity, and visual complexity. J Exp Psychol Hum Learn. 1980; 6:174–215. [PubMed: 7373248]

Sommer T, Rose M, Weiller C, Buchel C. Contributions of occipital, parietal and parahippocampal cortex to encoding of object-location associations. Neuropsychologia. 2005; 43:732–743. [PubMed: 15721186]

Suthana NA, Donix M, Wozny DR, Bazih A, Jones M, Heidemann RM, Trampel R, Ekstrom AD, Scharf M, Knowlton B, Turner R, Bookheimer SY. High-resolution 7T fMRI of Human Hippocampal Subfields during Associative Learning. J Cogn Neurosci. 2015a; 27:1194–1206. [PubMed: 25514656]

Suthana NA, Parikshak NN, Ekstrom AD, Ison MJ, Knowlton BJ, Bookheimer SY, Fried I. Specific responses of human hippocampal neurons are associated with better memory. Proc Natl Acad Sci U S A. 2015b; 112:10503–10508. [PubMed: 26240357]

Tkác I, Gruetter R. Methodology of1H NMR spectroscopy of the human brain at very high magnetic fields. Applied Magnetic Resonance. 2005; 29:139–157. [PubMed: 20179773]

Wadehra S, Pruitt P, Murphy ER, Diwadkar VA. Network dysfunction during associative learning in schizophrenia: Increased activation, but decreased connectivity: an fMRI study. Schizophr Res. 2013; 148:38–49. [PubMed: 23759649]

Woodcock EA, Wadehra S, Diwadkar VA. Network Profiles of the Dorsal Anterior Cingulate and Dorsal Prefrontal Cortex in Schizophrenia During Hippocampal-Based Associative Memory. Front Syst Neurosci. 2016; 10:32. [PubMed: 27092063]

Woodcock EA, White R, Diwadkar VA. The dorsal prefrontal and dorsal anterior cingulate cortices exert complementary network signatures during encoding and retrieval in associative memory. Behav Brain Res. 2015; 290:152–160. [PubMed: 25960314]

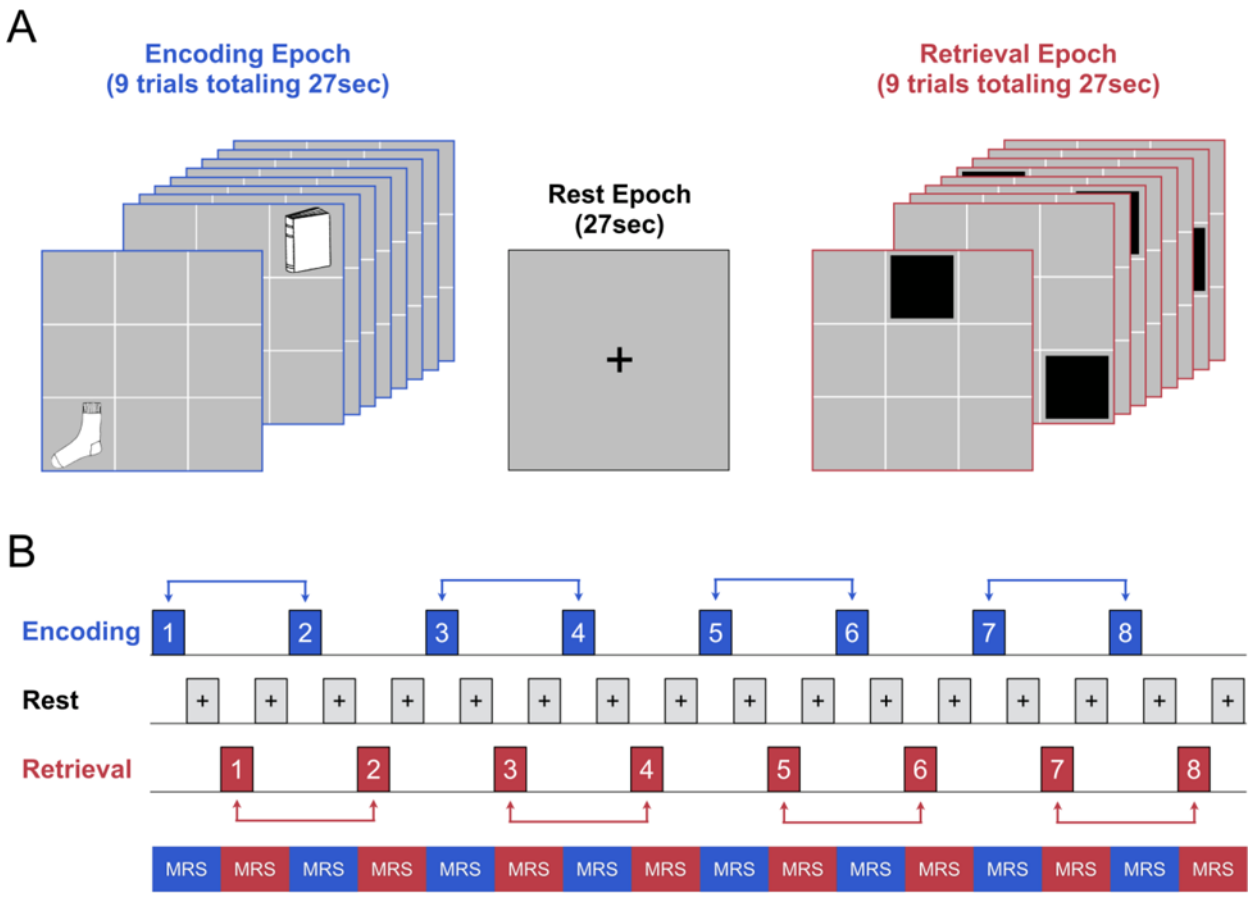

Figure 1.

(A) Schematic illustration of the associative learning and memory paradigm depicts the two-dimensional grid and example objects presented during encoding, and the cued locations during retrieval. The intervening rest epoch is depicted by fixation marker. The figure highlights the encoding and retrieval trials within their respective epochs, and the interspersed rest epochs. (B) A total of eight encoding and retrieval epochs were employed. As depicted, for ^{1}H MRS analyses, signals were averaged over successive encoding and retrieval epochs (paired arrows) to enhance SNR, resulting in four time points over which glutamate dynamics were assessed (see Figures 6 and 7). The timing of the individual ^{1}H MRS measurements is depicted along the bottom.

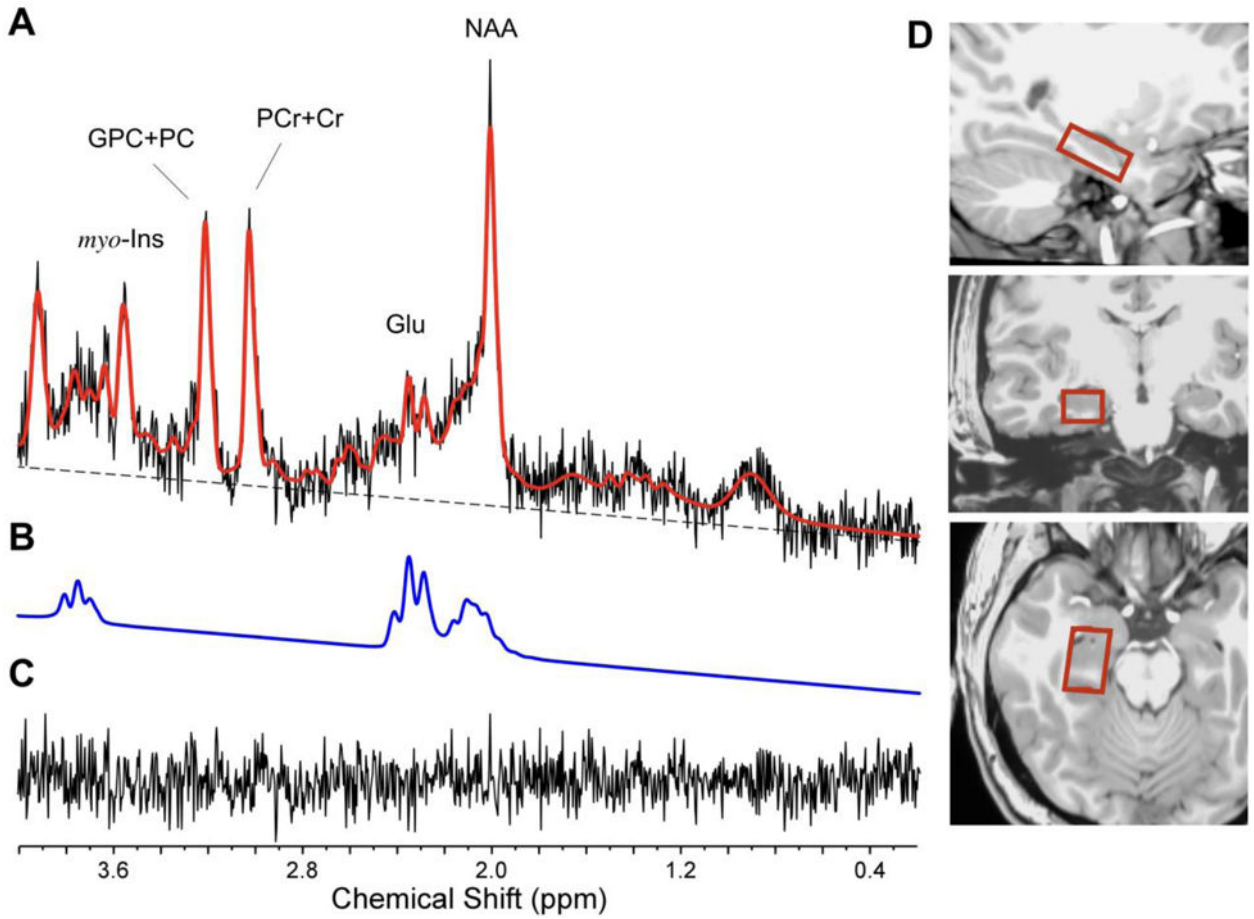

Figure 2.

(A) A typical example of an individual quantified ^{1}H MRS spectrum acquired in 54s (acquired in black and modeled spectrum in red). (B) Illustrates the signal of glutamate with a CRLB value of 8%. (C) The residual or difference between the acquired and modeled spectrum. (D) From top to bottom, the sagittal, coronal and axial view of the MRS voxel placed in the head/body of the hippocampus superimposed on the MRI.

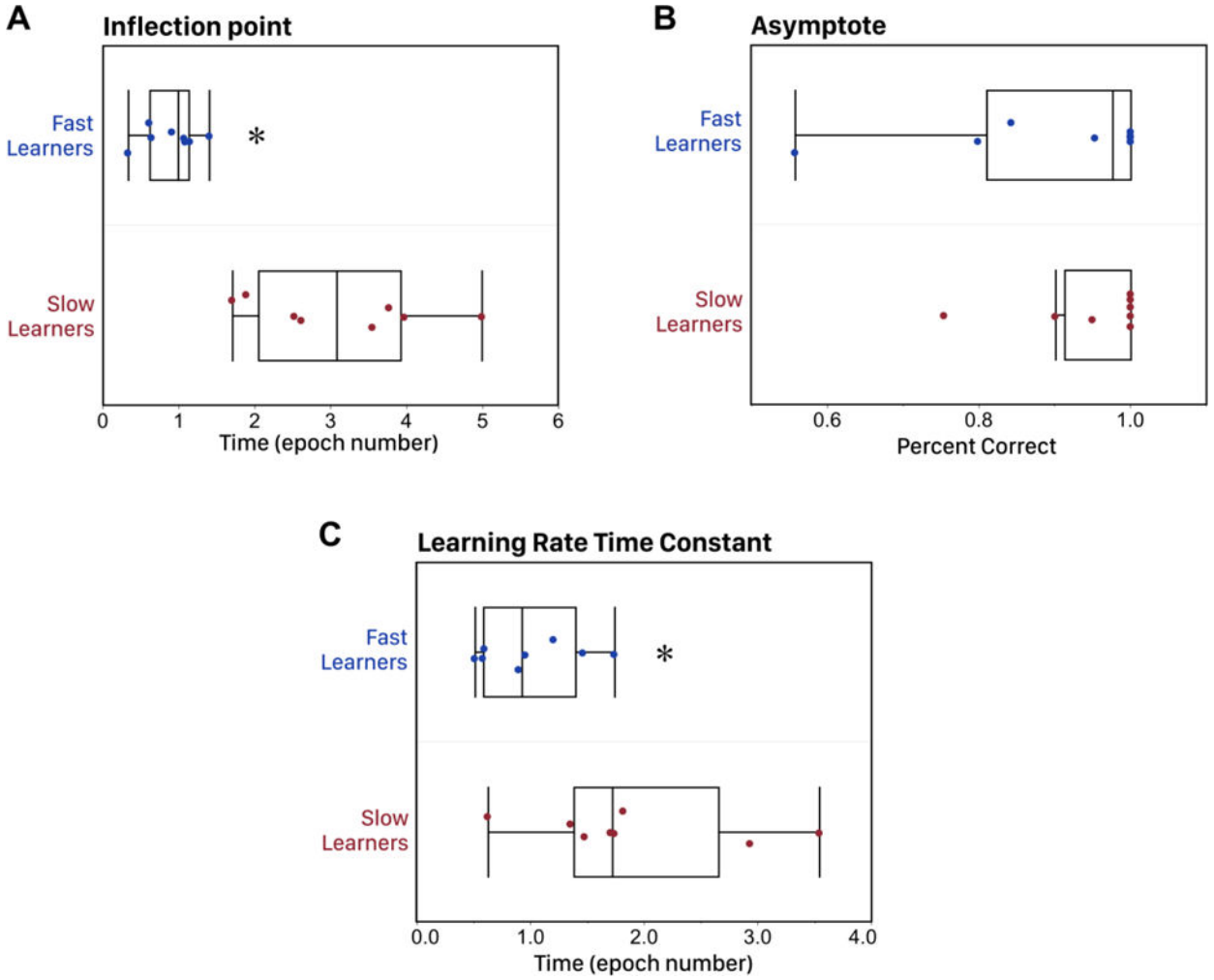

Figure 3.

Figures depict data modeled using the Gompertz function (see Methods). (A) Mean inflection points in time are plotted as boxplots demonstrating earlier task transition in fast (blue), relative to slow (red) learners. The color scheme is maintained throughout. (B) There were no significant differences in asymptotic performance across the learning sub-groups. (C) The learning rate time constant was significantly higher in fast, relative to slow learners.

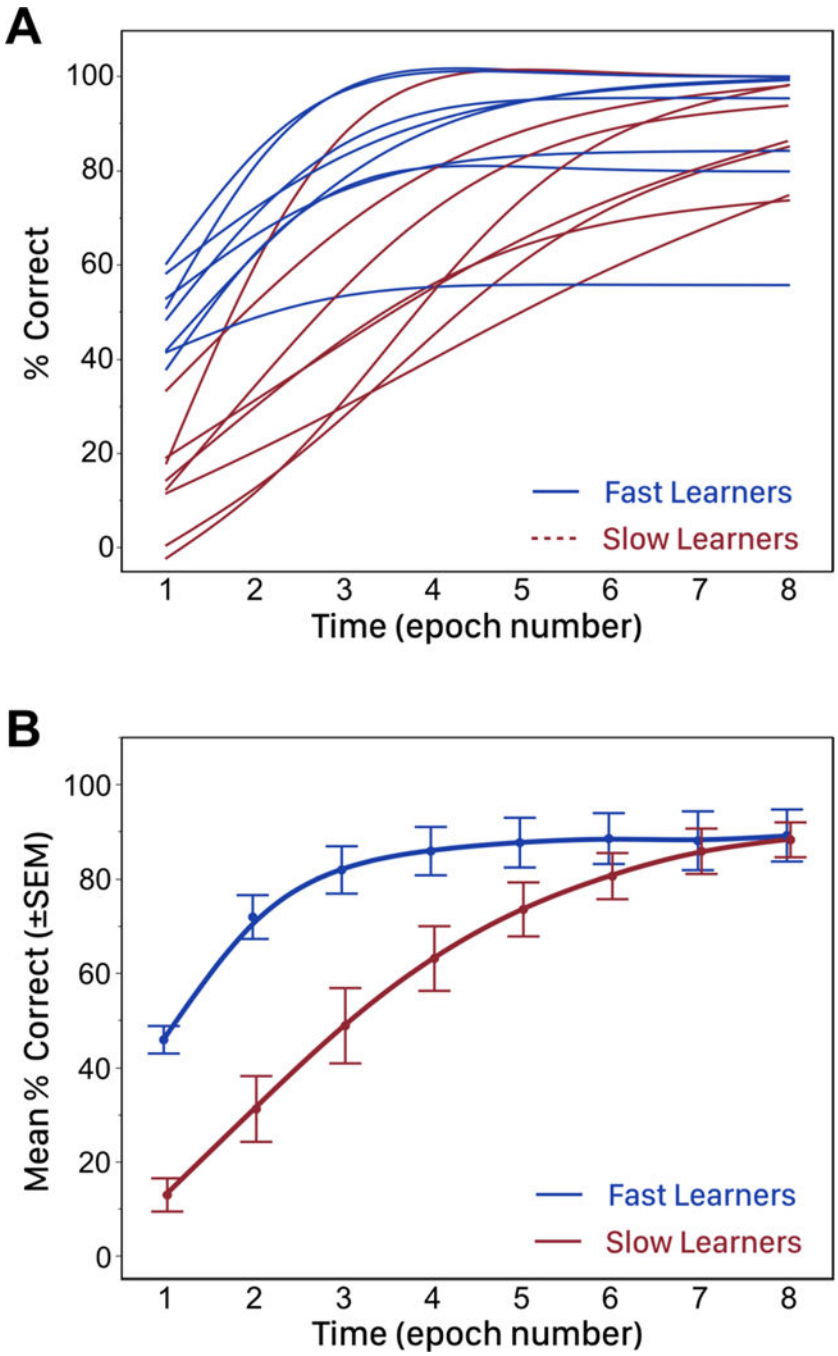

Figure 4.

Figures depict data modeled using the Gompertz function (see Methods). Raw behavioral performance (represented here for each of the eight epochs) plotted for each individual (A). (B) Raw behavioral performance (represented here for each of the eight epochs) is plotted as a function of learning group, depicting differential performance between fast and slow learners.

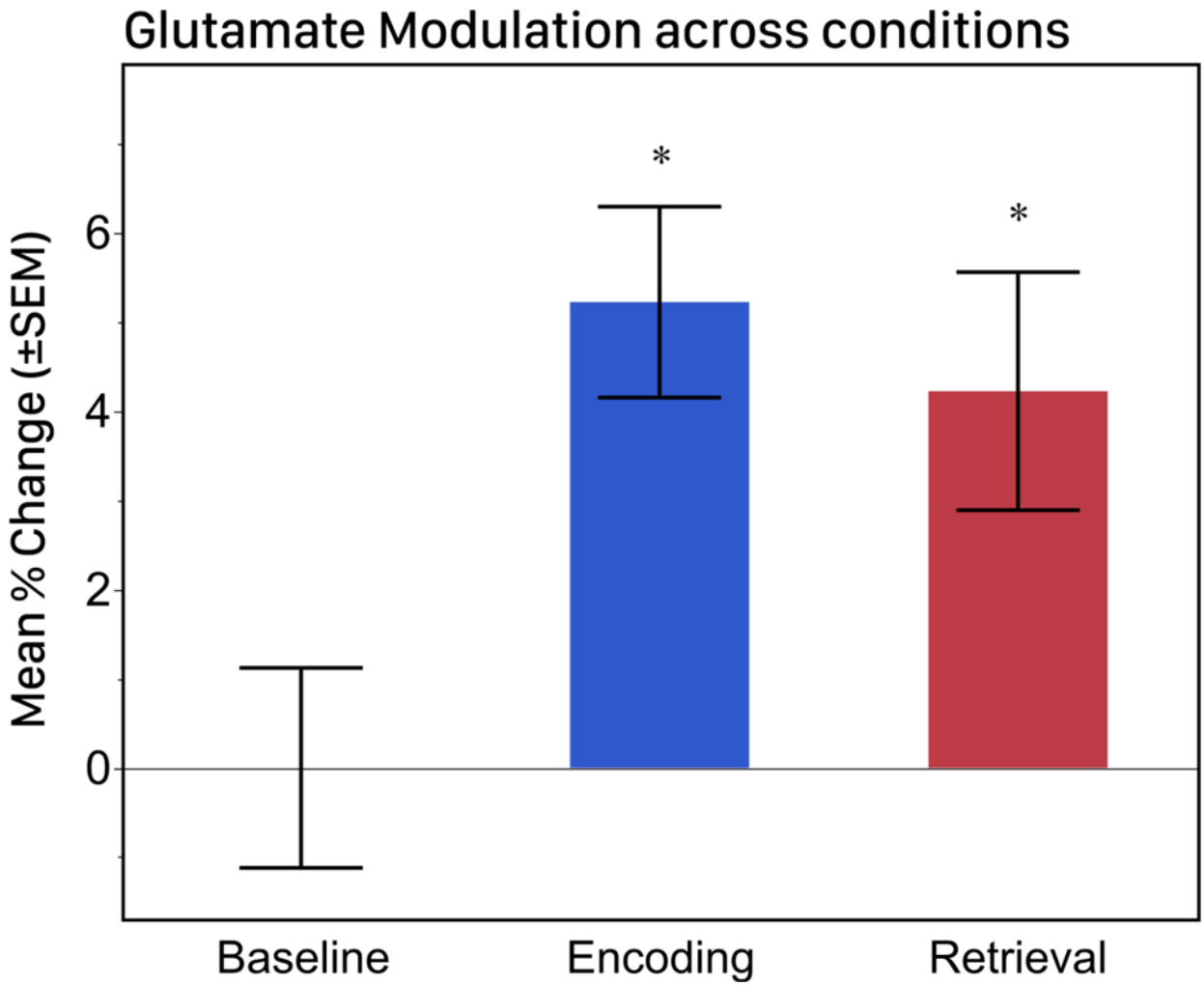

Figure 5.

The bars for each of the task conditions (encoding and retrieval) represent mean % levels of hippocampal glutamate relative to the control condition. The task condition term was significant with post-hoc analyses showing a significant increase in glutamate levels during both encoding ($p<0.0001$) and retrieval ($p=0.0002$).

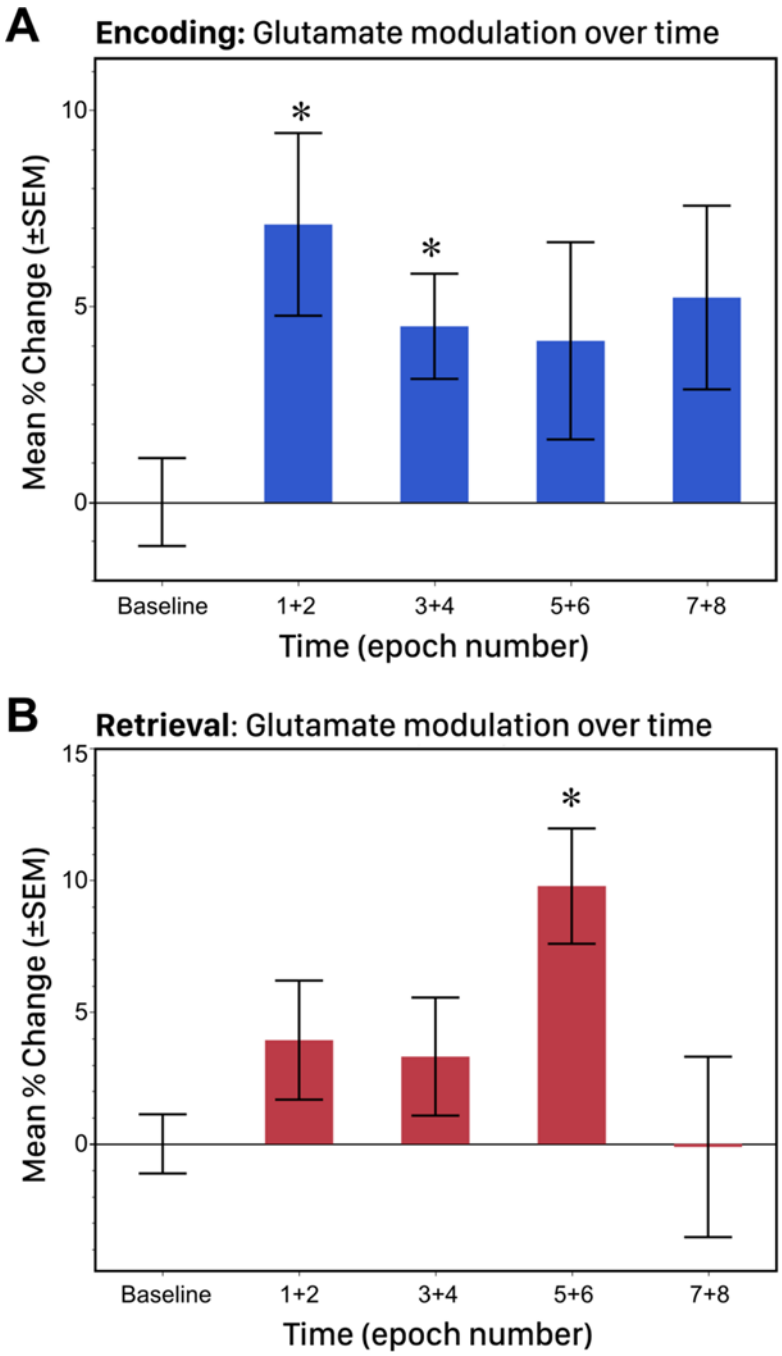

Figure 6.

Mean % levels of hippocampal glutamate across the paired epochs (see Figure 1) for the encoding (A) and retrieval (B) condition. Post-hoc analyses showed significant differences at multiple paired epochs during encoding and only in the 3rd paired epoch during retrieval both compared to the baseline condition, which are indicated by the "*".

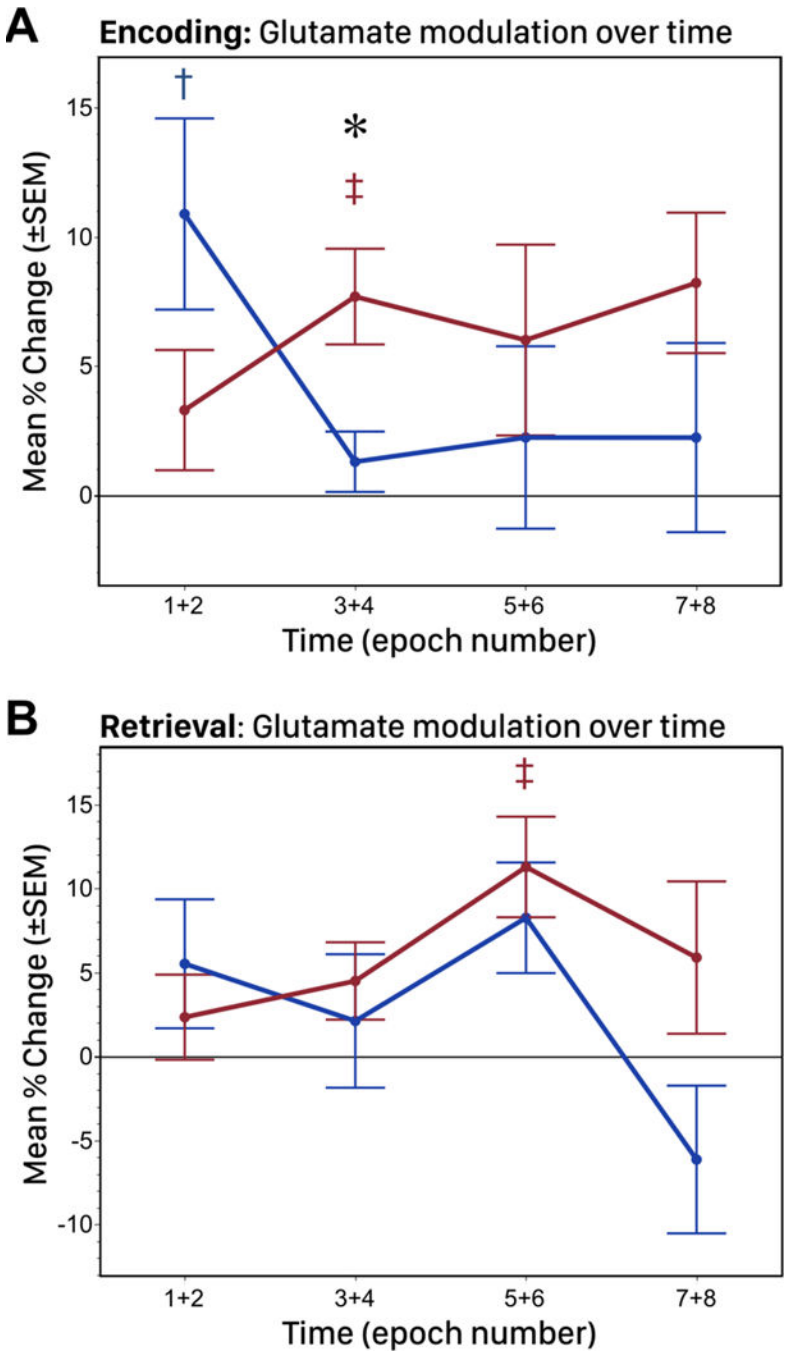

Figure 7.

Mean % levels of hippocampal glutamate across encoding (A) and retrieval (B) epochs for each of the learning groups. Significant differences in glutamate levels relative to the control condition are indicated for the fast (†) and slow (‡) learners as well as the significant difference between the fast and slow learners (✻).